Journal of
Ceramic Science
and Technology

J. Ceram. Sci. Tech., 07 [03] 277-288 (2016)
DOI: 10.4416/JCST2016-00016
available online at: http://www.ceramic-science.com

Sintering Behaviour of Fine Barium Titanate ($BaTiO_3$) Powders Consolidated with the Pressure Filtration Method

Ł. Zych*, A. Wajler, A. Kwapiszewska

AGH – University of Science and Technology, Faculty of Materials Science and Ceramics, al. Mickiewicza 30, 30 – 059 Krakow, Poland

received 24. Oktober 2015; received in revised form 5. Mai 2016; accepted 22. Mai 2016

Abstract

Main aim of the study was the determination of the sintering behaviour of fine barium titanate powders consolidated with the pressure filtration method. Three commercial powders with primary particle size of 50, 100 and 200 nm were used. Relationships between particle size, characteristics of the consolidated bodies and their sintering behaviour were investigated. The far-reaching goal of the study was the production of transparent or translucent barium titanate, a material that is part of a group of transparent ferroelectric ceramics applied in electro-optical devices. Aqueous and propanol suspensions of the powders were prepared and pressure-filtered at 10 MPa. Materials consolidated from the aqueous suspensions showed more advantageous pore size distributions, i.e. smaller modal pore diameter and lower total pore volume than those formed from the propanol suspensions and materials formed by means of cold isostatic pressing of the powders at 120 MPa. This was attributed to the smaller size of particles present in the aqueous suspensions compared with those in the propanol suspensions. Onset of the sintering process observed in dilatometric measurements was at 900 – 950 °C. The highest densities of approx. 98 % were achieved with sintering at 1300 °C or 1350 °C in air. Density exceeding 99 % was achieved by sintering with the SPS method at 1100 °C. Transmittance of the sample reached 55 % in the near-IR region.

Keywords: Barium titanate, nanopowder, pressure filtration, sintering, transparent ferroelectric ceramics

I. Introduction

Transparent ferroelectric materials are widely used in electro-optical devices including digital light modulators, optical shutters and switchers and image memory devices [1]. Among these materials, transparent ferroelectric ceramics (TFC) are of great interest on account of their many advantages such as lower production cost and ease of fabrication in a wide variety of sizes and shapes with good compositional control, compared to single-crystal materials. Transparent polycrystalline perovskite ceramics were discovered in the late 1960s as a result of a study on optimal processing and doping parameters for the lead zirconate titanate (PZT) system [2]. The best-known and commercialized TFCs are those from the lanthanum-modified lead zirconate titanate (PLZT) solid solution system [3].

However, up to now mostly lead-containing transparent ceramics, such as above-mentioned PLZT, $PbZrO_3$-$PbTiO_3$– $Pb(Zn_{1/3}Nb_{2/3})O_3$ (PZT-PZN), and $PbZrO_3$-$PbTiO_3$-$Pb(Ni_{1/3}Nb_{2/3})O_3$ (PZT-PNN), have been prepared [1]. For the environmental protection reasons, there is a need to replace the lead-based materials with more environmental-friendly ones, and lead-free transparent ferroelectric ceramics are much more desirable. However, reports on their preparation are rare and the fabrication of lead-free transparent ferroelectric ceramics is still a challenging issue. In the work of Wu and co-authors [4], barium strontium titanate (BST) powders were prepared using the conventional solid-state reaction method and sintered by means of spark plasma sintering. As a result, BST translucent ceramics (the transmittance in the visible light range of 0.3-mm-thick samples varied from about 40 % to 80 %) with average grain sizes of 880 nm – 1050 nm were prepared. Lead-free transparent electro-optic ceramics $(K_{0.5}Na_{0.5})_{1-x}Li_xNb_{1-x}Bi_xO_3$ have been fabricated by means of hot-press sintering and pressure-free sintering by Li and Kwok [5,6]. In their works, the ceramics' optical transmittance reached a value of 60 – 70 % in the near-IR region. Despite the fact that barium titanate (BT) is one of the most extensively studied and widely utilized perovskite-type ferroelectric materials, to our knowledge only two articles concerning translucent BT ceramics have been published to date. The first one was the work of Shimooka *et al.* [7], who used the sol-gel method to form partially crystallized $BaTiO_3$ monolithic xerogels and obtained translucent 85-%-density materials after sintering at 1100 °C in air. Liu *et al.* [8] prepared $BaTiO_3$ and $SrTiO_3$ ceramics by means of spark plasma sintering using commercially available nanopowders. In their work, translucent nanoceramics (grain size below 200 nm) with 99.2 % or 99.3 % theoretical density were fabricated.

* Corresponding author: lzych@agh.edu.pl

Main aim of the study is the determination of the sintering behaviour of fine $BaTiO_3$ powders consolidated with the pressure filtration method. The method belongs to a group of colloidal shaping techniques that can be successfully used for the consolidation of fine ceramic powders [9,10,11]. Three commercial powders with nanometric and submicron particle size were applied. Powders with various particle sizes were used in order to find relations between the particle size, characteristics of consolidated green bodies, their sintering behaviour and properties of the final materials. Results of the study may aid selection of the most suitable powder for colloidal processing. Far-reaching goal of the investigations is the production of translucent or transparent $BaTiO_3$ ceramics using the pressure filtration method.

There have been several studies on suspension preparation and colloidal consolidation of fine BT powders [12–21]. Fine barium titanate powders have been consolidated with colloidal methods such as slip casting [21], gel casting [18] or tape casting [15,17].

Pressure filtration of fine BT powders has been used in order to investigate effects of interactions between powder particles on their consolidation [12] or as a preliminary step of consolidation of a nanometric BT powder [16]. The pressure filtration method is suitable for effective consolidation of suspensions of fine barium titanate powders, because it may lead to homogeneous packing of the particles and does not require suspensions with high solid loading. Production of such suspensions in the case of barium titanate encounters problems [22]. The key issue here is the preparation of suspensions composed of as fine particles as possible, usually agglomerates, because their diameter corresponds to size of pores created between them, which in turn may influence the sintering behaviour of such material.

II. Experimental Procedure

(1) Starting materials and their characterisation

Three commercially available $BaTiO_3$ powders of different crystallite size (Inframat Advanced Materials LLC) were used. According to the producer, the average particle size of the powders was 50 nm (5622ON-N2), 100 nm (5622ON-01), and 200 nm (5622-ON2), and in the further text they will be denoted as I50, I100 and I200, respectively. According to the producer's characteristics, purity of the powders was 99.95 %. Particle sizes of the powders were determined using various methods. Phase composition of the powders was analysed using the x-ray diffraction method (XRD, Empyrean, PANanalytical).

The crystallite size (d_{XRD}) was calculated using Scherrer's formula on the basis of broadening of the (111) diffraction line. The specific surface area (SSA) was determined from the nitrogen adsorption isotherm and with the BET method (Nova 1200e, Quantachrome Inc.), and the results were used to calculate the diameter of an equivalent sphere (d_{BET}). The primary particle diameter (d_{TEM}) was determined from transmission electron microscopy observations (TEM, JEM 1011, Jeol Inc.). The diameter was calculated as a weighted average of at least 50 diameters of single particles of a given powder. The standard deviation was used as a measure of the distribution width. The diameter of each particle was measured in two perpendicular directions, and an average was calculated.

(2) Suspension preparation

The powders were consolidated using the pressure filtration technique (denoted **PF** in the text) which is one of colloidal shaping methods based on powder suspensions. Thus, in order to find the best conditions for the stabilization of the suspensions, a relation between the zeta potential and pH was determined (Zetasizer, Nano-ZS, Malvern Inc.). The measurements were performed on diluted suspensions containing 0.01 mol/dm^3 of NaCl. The pH was controlled using solutions of HCl (POCh, Poland) and NaOH (POCh, Poland). Suspensions were also prepared with the addition of Darvan C-N dispersing agent (Vanderbilt Minerals, LLC) in 3 wt% relative to the dry powder. The dispersing agent is a polyelectrolyte based on a water solution of ammonium salt of polymethacrylate, which proved to be an effective dispersant of BT powders [23]. To maximise effectiveness of the dispersing agent, the pH of the suspension was changed to 12 at which the highest values for the zeta potential of such system occur. Moreover, it is known that at pH < 7 barium titanate become unstable due to, amongst other things, a significant leaching of Ba^{2+} [22,24,25]. The pH was set at 12 using tetramethyloammonium hydroxide (TMAH, Acros organics) since it is an alkali-free base that can be removed without a trace during heat treatment of the material. TMAH in combination with ammonium polymethacrylate may lead to higher stability of barium titanate powders suspension as was observed in the case of barium zirconate suspensions [26].

Such conditions were chosen for the preparation of the water-based suspensions. In order to exclude the possibility of reactions between water and the $BaTiO_3$ powders, they were also dispersed in propanol (a.p., POCh, Poland). All suspensions were prepared by means of high-energy agitation (180 W) for 3 min using an ultrasonic disintegrator (UD-20, Techpan, Poland). The particle size distribution of powders in slightly diluted suspensions prepared for consolidation were measured with the Dynamic Light Scattering method (DLS, Zetasizer Nano-ZS, Malvern Inc.). The method is suitable for particles with a size up to about 6 μm. Modal particle diameters (d_{LD}) of the particle size distributions were determined.

The suspensions were consolidated using a pressure filtration method in a hydraulic, manual filter press made of a steel cylinder measuring 30 mm in diameter. Maximum possible volume of filtrated suspension was 70 cm^3. The suspensions were pressed with a steel piston against a porous ceramic support (filter) covered with a filter paper and nylon membrane with 0.2 μm pore size (Whatman). Pressure was increased up to 10 MPa and kept constant until supernatant leakage terminated. More details of this method are described elsewhere [11]. The green bodies produced had a diameter of 30 mm and a thickness of 5 mm. The green bodies were dried at room temperature in a desiccator over silica gel for 48 h and then in an oven at 105 °C for 6 h. In order to determine the effectiveness of the pressure filtration method, a number of reference samples of all

powders were produced by means of cold isostatic pressing at 120 MPa (denoted by **ISO** in the text). The pore size distribution of the materials was determined with the mercury porosimetry method (Poremaster 60, Quantachrome Inc.). In order to exclude effects of the presence of some organics in the samples that may influence their pore size distribution, the measurements were performed on samples fired at 900 °C for 30 min.

(3) Sintering

The sintering process was investigated based on heating of the samples in a dilatometer (Netzsch DIL 420 C) up to 1350 °C with a heating rate of 5 K/min. The filter-pressed samples and the reference samples were sintered in air in a laboratory electric furnace (LHT 04/18, Nabertherm) at 1200, 1250, 1300 and 1350 °C for 1 h with a heating rate of 5 °C/min. The selected sample was sintered using a spark plasma sintering furnace type HP D5 (FCT Systeme GmbH) at 1100 °C for 5 min with a heating rate of 100 K/min in vacuum. During the SPS sintering, the sample was pressed in a graphite die under a pressure of 30 MPa.

(4) Characterisations

The apparent density of the sintered samples was determined using the Archimedes method. The true density of $BaTiO_3$ used in calculations was 6.02 g/cm^3. The microstructure of the sintered materials was observed using scanning electron microscopy (Nova Nano-SEM 200, FEI Co). The observations were performed on polished surfaces. The samples were thermally etched at 1250 °C for 6 h in air. In the case of the SPS-sintered sample, its fracture surface was observed. Phase composition of selected sintered samples was analysed with the XRD method (Empyrean, PANanalytical). Optical transmission in the infrared and visible light range was measured on a double-side-polished sample of 1 mm in thickness by a Varian Cary 500 spectrophotometer. Before the measurement, the sintered sample was annealed at 900 °C for 6 h in order to ensure full oxidation.

III. Results and Discussion

(1) Powders and suspension characteristics

According to XRD results, all powders consisted only of tetragonal phase of $BaTiO_3$. The powders had tetragonal symmetry, which meant that in order to produce transparent or at least translucent ceramics, the material ought to be fully dense with a microstructure consisting of grains of submicron size. For example, for hexagonal alumina (corundum) such a grain size was between 0.5 and 0.8 μm. Transmittance of such aluminas in optical range was approx. 50 % [27,28]. Crystallite sizes (d_{XRD}) of the powders determined from the XRD measurements generally matched with the producer's characteristics (Table 1). Particle diameters calculated on the basis of specific surface area (d_{BET}) were similar to values of the XRD crystallites size (d_{XRD}). The largest difference between the results occurred in the case of I100 powder, where d_{BET} was 94 nm and was larger than d_{XRD} equal to 78 nm. It may indicate the presence of some relatively broad phase contacts formed between individual crystallites within a powder agglomerate. Generally good consistence between d_{XRD} and d_{BET} in other two powders indicated that the powders consisted of agglomerates with small contacts between individual crystallites. Such agglomerates can be relatively easily broken down into smaller particles (smaller agglomerates rather than individual crystallites) during preparation of the powders suspensions, e.g. by ultrasonication or attrition milling. The particle size distribution of a powder in suspension used for consolidation affects the results of the process i.e. the properties of consolidated green body such as apparent density or pore size distribution. For this reason, it is vital to prepare suspensions consisting of particles that are as small as possible, especially in the case of fine powders, which are always agglomerated. Both d_{BET} and d_{XRD} should be treated as kind of mean values, which only estimate the size of the primary particles of the powders.

More direct characterisation of the powders morphology was possible with the TEM observations. All powders had similar morphology and they only differed in their primary particle (crystallite) size. As an example, a TEM microphotograph of I100 powder is shown in Fig. 1. The TEM observations of the powders generally confirmed the results of d_{XRD} and d_{BET} analysis. All powders consisted of round crystallites gathered in rather loose agglomerates. In all powders, a primary particle diameter determined from the TEM observations (d_{TEM}) was larger than d_{XRD} and d_{BET} (Table 1). One possible cause of such differences was the fact that mean primary particle (crystallite) sizes determined from SSA or XRD analysis are generally related to smaller particles. From the principle, they should make a greater contribution to both SSA and x-ray diffraction line broadening than larger crystallites (particles). Moreover, according to the TEM observations the powders had relatively broad distribution of the crystallite diameter (Table 1), so it was more probable that the mean values, i.e. d_{BET} and d_{XRD} would be different from d_{TEM} value.

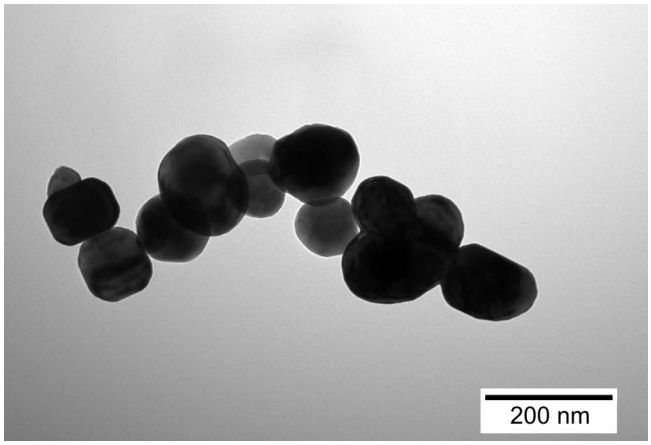

Fig. 1: TEM microphotographs of I100 powder.

Generally, such submicron powders sinter more efficiently than nanometric ones, leading to denser materials with fine microstructure. Processing of submicron powders is also easier since agglomerates formed by such powders have lower strength than agglomerates of nanometric powders and thus they could be broken down relatively easily [9]. Particle diameters measured in the real suspensions (d_{LD}) were larger than diameters of the primary

Table 1: Characteristics of the $BaTiO_3$ powders.

Powder name	I50	I100	I200
Phase composition	100 % tetragonal $BaTiO_3$	100 % tetragonal $BaTiO_3$	100 % tetragonal $BaTiO_3$
Specific surface area, m^2/g	21.3	10.6	4.9
d_{BET}, nm	47	94	201
d_{XRD}, nm	44	78	206
d_{TEM}, nm	70	126	223
d_{LD} *) (water), nm	140	190	350
d_{LD} *) (propanol), nm	825	340	460
Isoelectric point, pH	3.4	4.4	4.2

*) modal value of the particle size distribution measured by the DLS method

particle (d_{BET}, d_{XRD} and d_{TEM}) (Table 1), which is discussed in a further part of the paper. The relation between the zeta potential and pH of the suspensions was similar for all powders (Fig. 2) with isoelectric point values between pH 3.4 and pH 4.4 for I50 and I100 powder, respectively (Table 1). Maximum absolute values of the zeta potential occurred between pH 2 and 3 and at pH 12. It is known that from the point of view of the suspensions' stability, absolute values of zeta potential should be higher than 30 mV [29]. For all investigated powders such values occurred at pH 12, where the zeta potential ranged from −30 to −45 mV for I50 and I200 powder, respectively (Fig. 2). Addition of ammonium polymethacrylate and adjustment to pH 12 using TMAH led to a substantial increase in the zeta potential values, which then ranged from −55 to −75 mV for I50 and I200 powder, respectively (Fig. 2). Suspensions prepared in such conditions were well dispersed and their consolidation by means of filter pressing should lead to green bodies with a homogeneous microstructure favourable for sintering [10,11].

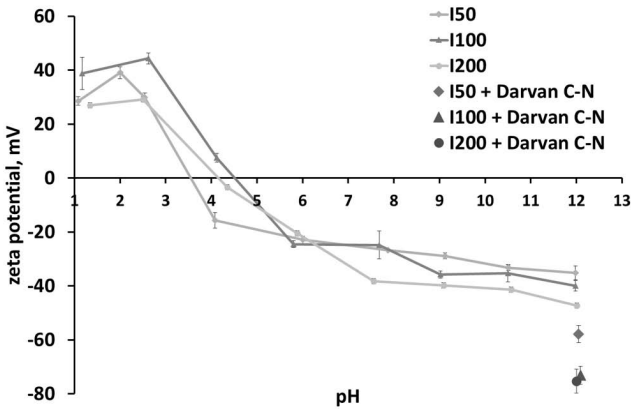

Fig. 2: Zeta potential of the $BaTiO_3$ powders vs. suspension pH.

The filter pressing method can be applied for the consolidation of low-solid suspensions, so the amount of the dispersing agent was not optimised based on an evaluation of the suspensions' rheology. The particle size distributions determined in the real suspensions were narrow, but they indicated that all powders were agglomerated (Fig. 3). Most of the agglomerates had diameters smaller than 1 μm, but larger agglomerates existed in almost every suspension. These would probably be broken down if a different method had been chosen for preparation of the suspensions, e.g. attrition milling. It should be noted the DLS method is suitable for particles with narrow size distributions and diameters smaller than approx. 6 μm. Larger particles existing in the suspension cannot be precisely measured but their presence interferes with the measurement.

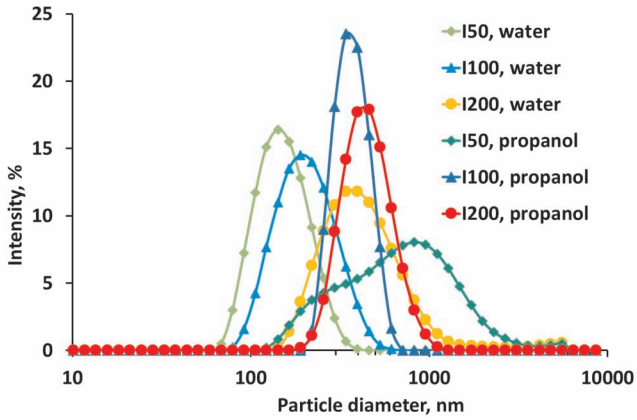

Fig. 3: Particle size distribution of the real $BaTiO_3$ suspensions (water and propanol).

Modal values of the particle size distributions of the water suspensions corresponded approximately to 1.5, 2.0, and 3.0 times the crystallite size (d_{XRD}) of the I200, I100 and I50 powders respectively (Table 1). It reflected a tendency of smaller particles (crystallites) to form relatively large agglomerates. The agglomerates of the powders formed in propanol were bigger than the ones present in the water suspensions (Fig. 3). Here the ratio of agglomerate diameter to the particle diameter was approximately 2, 4, and 18 for I200, I100 and I50 powders respectively (Table 1). There could be a few reasons for the differences observed between size of agglomerates present in water or propanol suspensions. Powders in the water suspensions were well stabilised with the addition of the dispersing agent and pH adjustment while in the case of the propanol suspensions the powders were not stabilised by any means. In the presence of the dispersing agent the agglomerates could be more easily broken down into smaller pieces. Lack of stabilisation could result in faster agglomeration of the powders and thus generally larger modal ag-

glomerate size. On the other hand, it should be noted that generally all powders were easily dispersed in propanol and, with the exception of powder I50, formed suspensions with a narrow particle size distribution suitable for consolidation by means of filter pressing or other colloidal shaping techniques.

(2) Characteristics of the consolidated samples

It was observed, that green samples prepared from the propanol suspensions exhibited lower mechanical strength that those prepared from the water suspensions. This can be attributed to the lower surface tension of propanol compared to water and thus the lower strength of contacts formed between the particles during drying. However, the strength of the propanol-suspension-derived samples was sufficient to manipulate them and no temporary binder was added during suspension preparation. Characteristics of the suspensions based on different solvents influenced their consolidation process by filter pressing, which could be observed from the pore size distributions of the pre-sintered samples (Fig. 4).

The pore size distributions of most samples were monomodal with the modal pore value ranging from approx. 80 to 280 nm, which tended to correspond to some fraction of the diameter of an agglomerate of a given powder rather than to its crystallite size (Fig. 3, Table 1). Samples consolidated from the water suspensions showed a pore size distribution that was more favourable from the point of view of the sintering process than the ones from the propanol suspensions. i.e. monomodal, narrow and with low total pore volume corresponding to a high apparent density of a material. In all cases, samples prepared from the propanol suspensions had a higher total pore volume (Fig. 4). This was especially visible in the case of those samples consolidated from I50 powder, where the total pore volumes were 107 and 217 mm^3/g for the water-suspension-based and the propanol-suspension-based samples, respectively (Fig. 4a).

The modal pore diameter in all propanol-suspension-based samples was larger than the one recorded in the water-suspension-based samples. For example, for samples prepared from I100 powder the modal pore diameters were 262 nm and 74 nm for the propanol-suspension- and water-suspension-derived samples, respectively. Additionally, in the propanol-suspension-based samples prepared from I100 and I200 powders, a small population of pores of a few micrometres in diameter appeared (Fig. 4b, c). Differences in the pore size distributions in samples prepared from different suspensions resulted from the much larger size of agglomerates present in the propanol suspensions (Fig. 3, Table 1). It means that forces acting during the filter pressing consolidation were not strong enough to deform the agglomerates from the propanol-based suspension and to pack them more densely. From the point of view of pore size distribution favourable for the sintering process, suspensions used for consolidation should exhibit narrow particle size distribution with as small a modal particle diameter as possible.

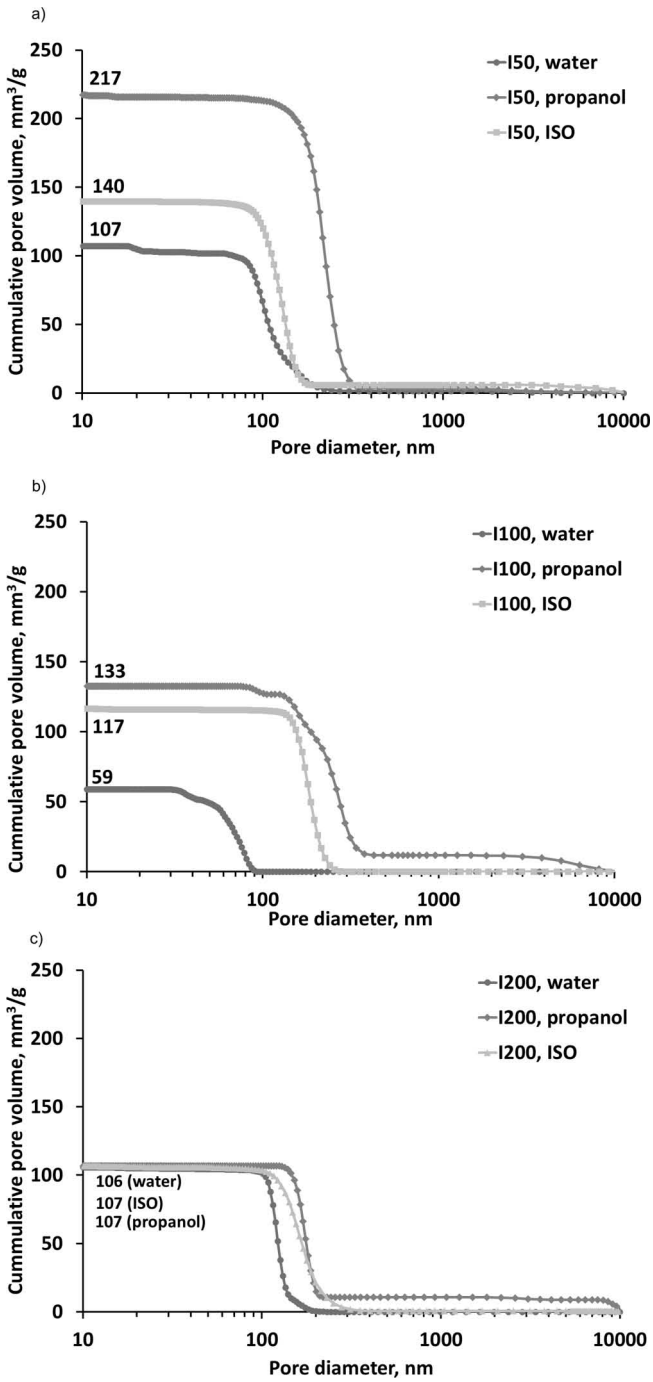

Fig. 4: Cumulative curves of the pore size distribution in samples pre-sintered at 900 °C; a) I50, b) I100, c) I200.

Filter pressing in comparison to other common colloidal consolidation techniques such as slip casting, or gel casting could be more effective in consolidation of fine powders because external pressure applied on consolidated suspension corresponds to relatively high force acting on a single particle. The results presented above showed that this force was strong enough to pack the agglomerates of both suspensions, but it could not deform/crush them. Otherwise, pore size distributions in samples prepared from water or propanol suspension of a given powder should be similar. Probably for this reason, the smallest differences between pore size distributions were observed in the case of samples prepared from I200 powder (Fig. 4c), whose modal particle diameter was similar in

water and propanol suspensions (Fig. 3, Table 1). In the case of these samples the total pore volume was 106 and 107 mm^3/g for water-suspension-derived, and propanol-suspension-derived samples, respectively (Fig. 4c). Modal pore diameter was 123 and 176 nm for the water-suspension-derived, and propanol-suspension-derived samples, respectively. Modal particle diameter was 350 and 460 nm in the water and propanol suspension, respectively. Larger differences in pore size distributions were observed in the case of samples prepared from finer and for this reason probably more agglomerated powders i.e. I50 (Fig. 4a) and I100 (Fig. 4b).

The effectiveness of the pressure filtration of the powders suspensions and cold isostatic pressing of the dry powders under 120 MPa (the pressure value was chosen for technical reasons) was compared based on the pore size distributions in both types of material. In all cases the cumulative pore volume in the cold-isostatic-pressed samples was higher than the pore volume of samples filter-pressed from the water suspensions, but lower than the pore volume of samples derived from the propanol suspensions (Fig. 4). Values of the modal pore diameters of the cold-isostatic-pressed samples were placed between values of modal pore diameters for the filter-pressed samples in a similar manner as the cumulative pore volume. Here also the smallest differences between pore size distribution of the dry-pressed samples and the filter-pressed samples were observed in the case of samples prepared from I200 powder (Fig. 4c). It only proved that I200 powder consisted of relatively weak agglomerates that were broken down during suspension preparation to a minimum size.

Practically, such agglomerates could not be deformed further and for this reason their consolidation by different methods led to similar results i.e. pore size distributions (Fig 4). From the point of view of pore size distribution, the most effective method of consolidation was filter pressing of the water suspensions because it led to the lowest cumulative pore volume and the smallest modal pore diameter, which is favourable for the sintering process. The less effective method was filter pressing of the propanol suspensions, because, apart from the highest values of both the cumulative pore volume and the modal pore diameter, also some large pores appeared, which could have a detrimental effect on the sintering process. Origin of the large pores was not clear, but their size and relatively low volume (Fig. 4b, c) indicated that they tended to be cracks created during drying of the samples rather than inhomogeneities resulting from packing of the agglomerates, which had narrow size distribution (Fig. 3) during the filter pressing.

(3) Sintering process

Dilatometric curves of the materials are shown in Fig. 5. For all samples, distinct shrinkage started in a temperature range of 900 – 950 °C, and it can be attributed to an onset of the sintering process. Measured linear shrinkage ranged from 28.2 % to 16.6 % for I50 (propanol) and for I200 (iso) samples, respectively. Generally, the highest shrinkage occurred in samples derived from I50 powder (Fig. 5a) and the lowest in samples derived from I200 powder (Fig. 5c), which was roughly inversely proportional to the total pore volume (Figs. 4a, 4c), in other words more porous samples shrank more. This behaviour was especially visible in the case of samples filter-pressed from all propanol suspensions. The relative density of the filter-pressed samples isostatically sintered at selected temperatures is shown in Fig. 6. The majority of the materials reached the highest densities at 1300 °C or 1350 °C, and these temperatures were used as the final ones. The only exception was the sample prepared from the propanol suspension of I50 powder, which reached the maximum relative density i.e. 99.16 ± 0.25 % at 1250 °C, higher sintering temperatures leading to a distinct decrease in density (Fig. 6).

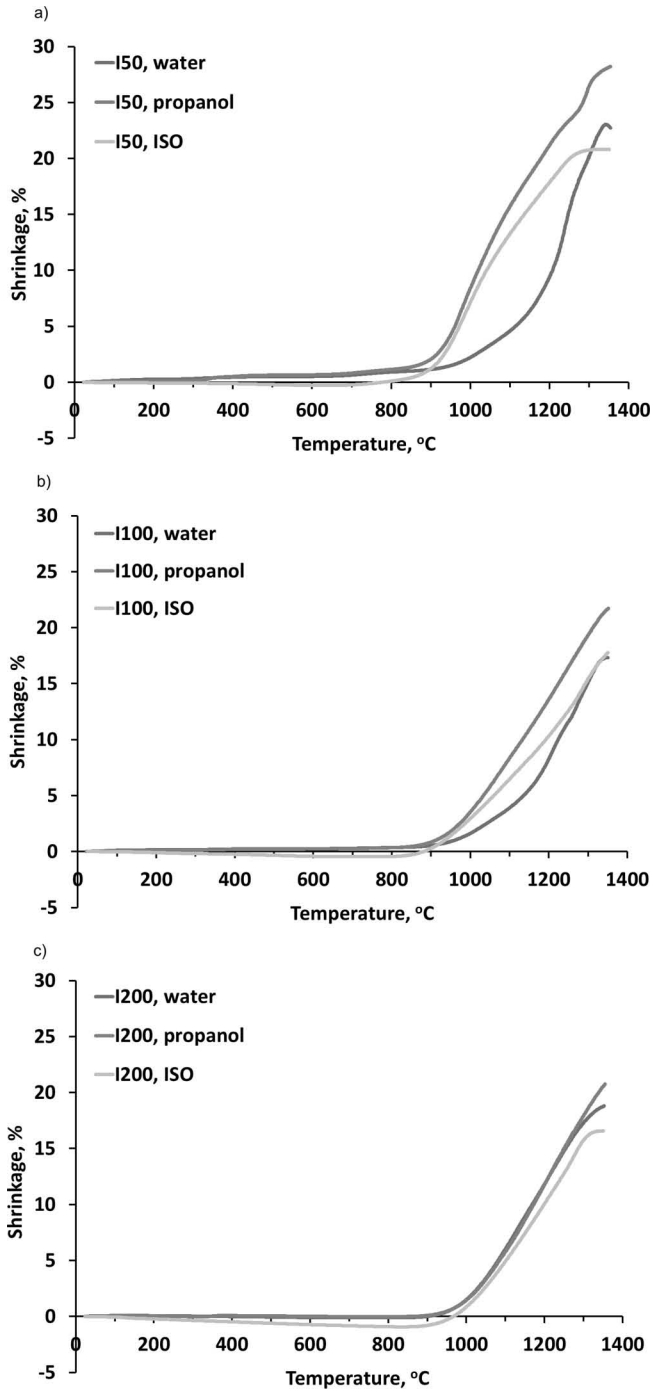

Fig. 5: Shrinkage of samples during sintering in a dilatometer; a) I50, b) I100, c) I200.

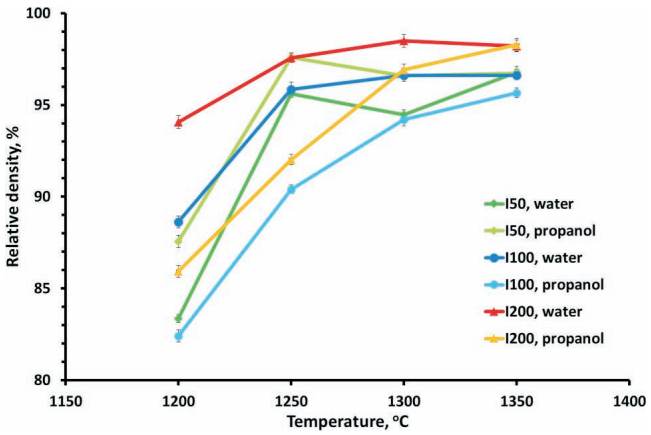

Fig. 6: Relative density of the filter pressed samples vs. sintering temperature.

The origin of this behaviour was not clear, especially as this sample had the less favourable pore size distribution i.e. the highest total pore volume and the modal pore diameter (Fig. 4a) originating from a rather wide particle size distribution (Fig. 3). One of possible explanations was that I50 powder consisted of the smallest particles and thus it could sinter and densify at lower temperatures than the other powders. Compared with other propanol-suspension-derived samples, here the pore size distribution was unimodal and the population of few-micron-size pores was absent (Fig. 4a). On the other hand, the modal pore volume of the propanol-suspension-derived samples was higher than that of the others (Fig. 4a), so it can be concluded that densification of samples prepared from I50 powder was not only related to the initial pore size distribution. A plausible explanation for the observed decrease in the density of some materials with increasing sintering temperature is provided in the further discussion.

It is interesting to note that samples prepared from different suspensions of a given powder reached similar densities after sintering at 1350 °C (Fig. 6). This may suggest that at this temperature some equilibrium state was reached. In order to compare the sintering behaviour of samples consolidated by means of different methods, samples prepared with cold isostatic pressing were also sintered at 1300 °C and 1350 °C. The relative density of all those samples did not exceed 99 % (Fig. 7). In most cases, samples of a given type showed the same or slightly higher densities when sintered at 1350 °C. Generally, the lowest relative densities were achieved by samples prepared from I50 powder and the highest by samples made of I200 powder. In those two powders, differences in densification between the filter-pressed and the isostatic-pressed samples were within approx. 1 % of the relative density. Cold isostatic pressing gave the best results in the case of I100 powder, samples consolidated with this method having significantly higher densities than samples prepared by means of filter pressing. It seems that in the case of samples prepared from I100 powder final densification did not depend on the initial pore size distributions relative to the consolidation techniques. Otherwise, samples filter-pressed from the water suspension would have the highest density, because pores present in such samples had much smaller diameter and total volume than the ones present in the cold-isostatic-pressed samples (Fig. 4b). A reason for the observed density differences between samples consolidated with various methods and the fact, that the maximum achieved densities did not exceed 99 % could be explained on the basis of microstructure observations.

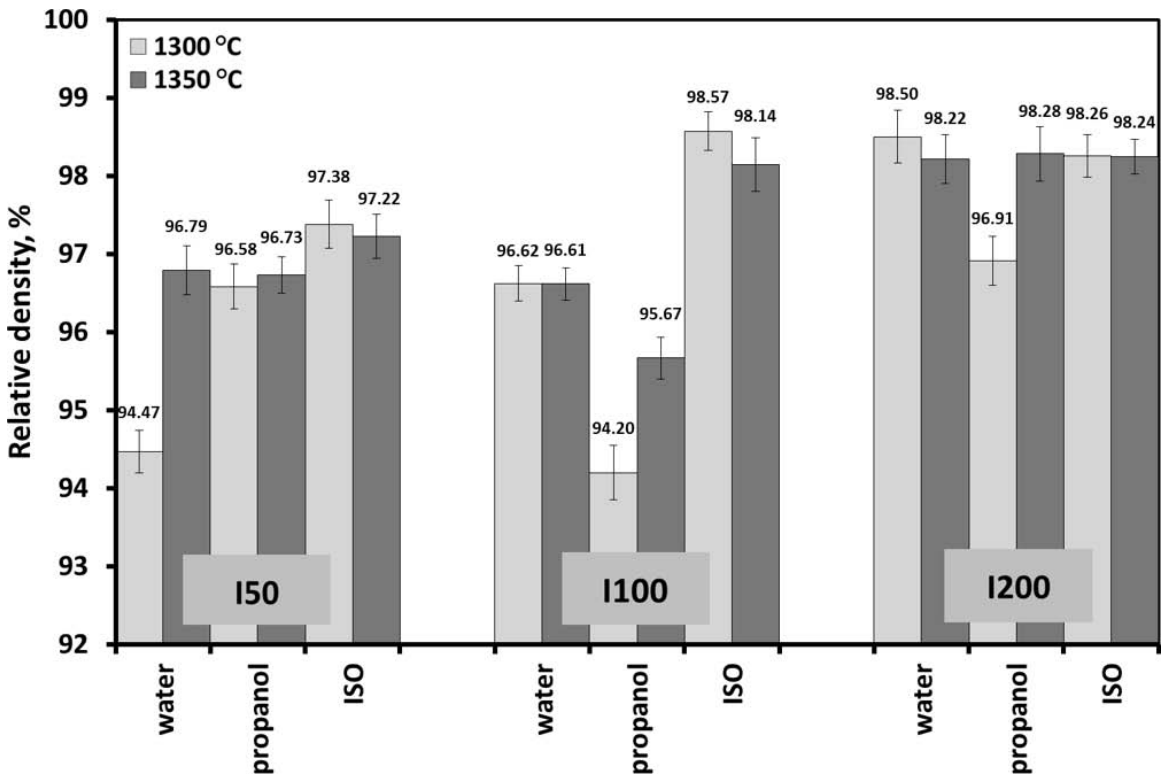

Fig. 7: Relative density of $BaTiO_3$ samples sintered at 1300 °C and 1350 °C.

(4) Microstructure

Microstructures of samples sintered at both temperatures showed similar features, and thus only microphotographs of samples prepared from I50, I100 and I200 powders and sintered at 1300 °C are presented in Figs. 8, 9, and 10, respectively. In most cases, the microstructure of densified samples derived from I50 powder consisted of large grains between 50 and 100 μm in size (Fig. 8). The general view of the microstructure did not depend on the consolidation technique and was similar for the pressure-filtered (Fig. 8c) and the isostatically pressed samples (not shown here). The most distinct features were closed pores present inside the grains, which is typical for barium titanate ceramics. Their presence precluded full densification of the materials, regardless of the grain size. The microstructure of a sample consolidated by means of filter pressing of a water suspension with relative density of 94.47 % (Fig. 7) consisted of large, porous grains (Fig. 8a) surrounded by sub-micrometric grains (Fig. 8b). A similar microstructure was observed in the case of a sample filter-pressed from a water suspension of I100 powder (Fig. 9a).

Relative density of the sample was 96.62 % (Fig. 7), and the smaller grains had a diameter of approx. 1 μm (Fig. 9b). Conversely, the microstructure of samples filter-pressed from the propanol suspension (Fig. 9c) as well as that of the isostatically pressed samples (Fig. 9d) was more uniform. In the case of a sample filter-pressed from the propanol suspension, most pores were located at grain boundaries (Fig. 9c) and their amount corresponded to its relatively low density of 94.20 % (Fig. 7).

The microstructure of the isostatically pressed sample from I100 powder (Fig. 9d) was similar to the one observed in samples filter-pressed (Fig. 8c) or isostatically pressed from I50 powder. The observed abnormal grain growth (Figs. 8a, b and 9a, b) is a typical, and usually unwanted behaviour of barium titanate, which can be attributed to the presence of inhomogeneously distributed small amounts of a liquid phase during sintering [30, 31]. In theory, the presence of sub-micrometric or micrometric grains in the relatively dense, water-suspension-derived samples prepared from I50 (Figs. 8a, b) and I100 (Figs. 9a, b) powder creates the opportunity to produce dense, fine-grained material using post-HIP treatment. The open question here is if it is possible to find sintering conditions at which all pores are closed and located at grains boundaries, and the microstructure consists only of the sub-micrometric grains. The microstructure of samples derived from I200 powder was similar irrespective of the consolidation method (Fig. 10). Generally, the microstructure of all the samples was uniform and consisted of large grains of approx. 20 to 50 μm in diameter with closed pores inside (Figs. 10a, b, c).

To conclude, after pressureless sintering neither the filter-pressed nor the cold isostatically pressed materials achieved full density and a microstructure consisting of fine grains, and thus the materials were opaque. Despite observed differences in the characteristics of green samples which were related to the consolidation process, the properties, i.e. density and grain size, of the sintered materials were very similar. This was caused by rapid grain growth leading to the adverse closure of pores inside the grains.

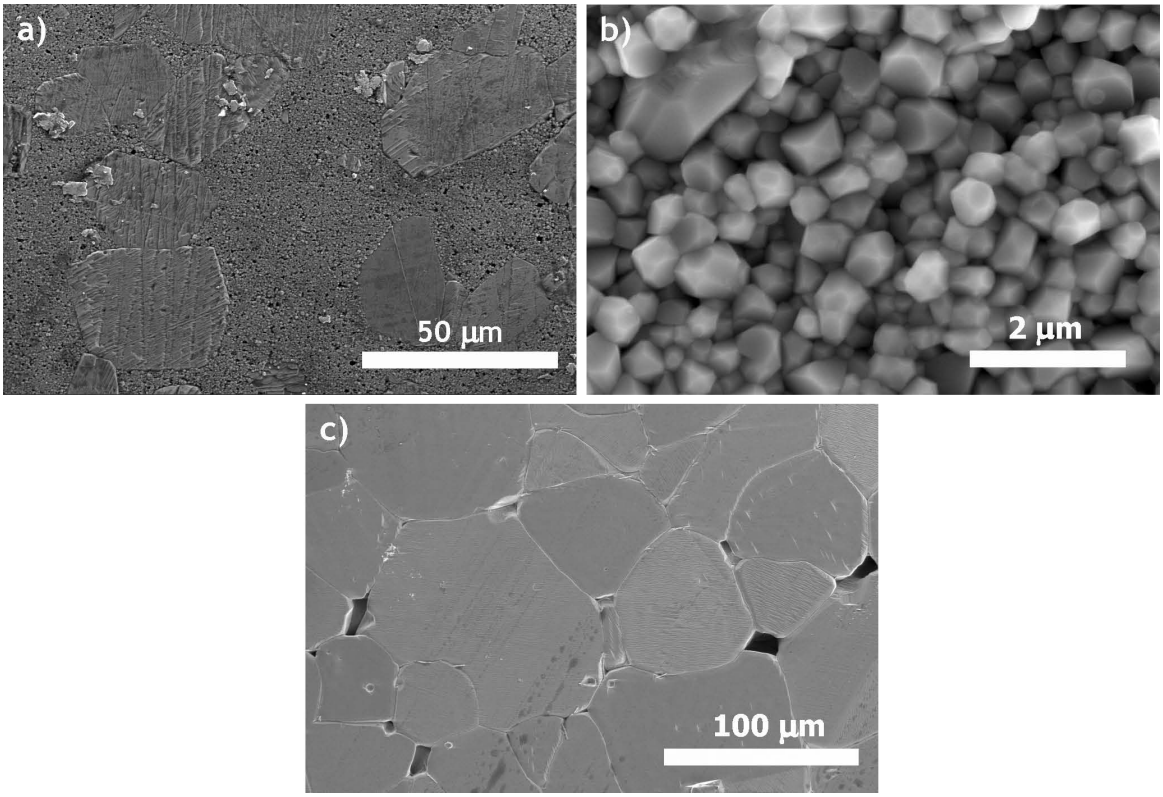

Fig. 8: SEM microphotographs of microstructure of samples prepared from I50 powder sintered at 1300 °C: a) PF, water; b) PF, water (different magnification); c) PF, propanol.

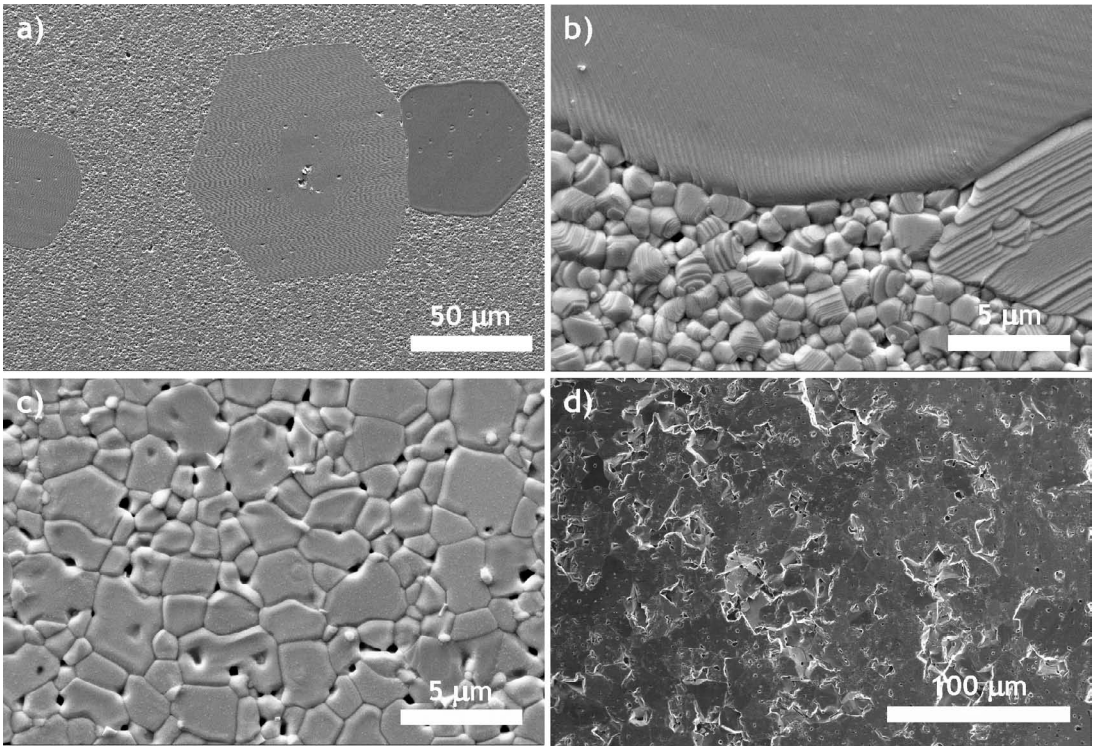

Fig. 9: SEM microphotographs of microstructure of samples prepared from I100 powder sintered at 1300 °C: a) PF, water; b) PF, water (different magnification); c) PF, propanol; d) ISO.

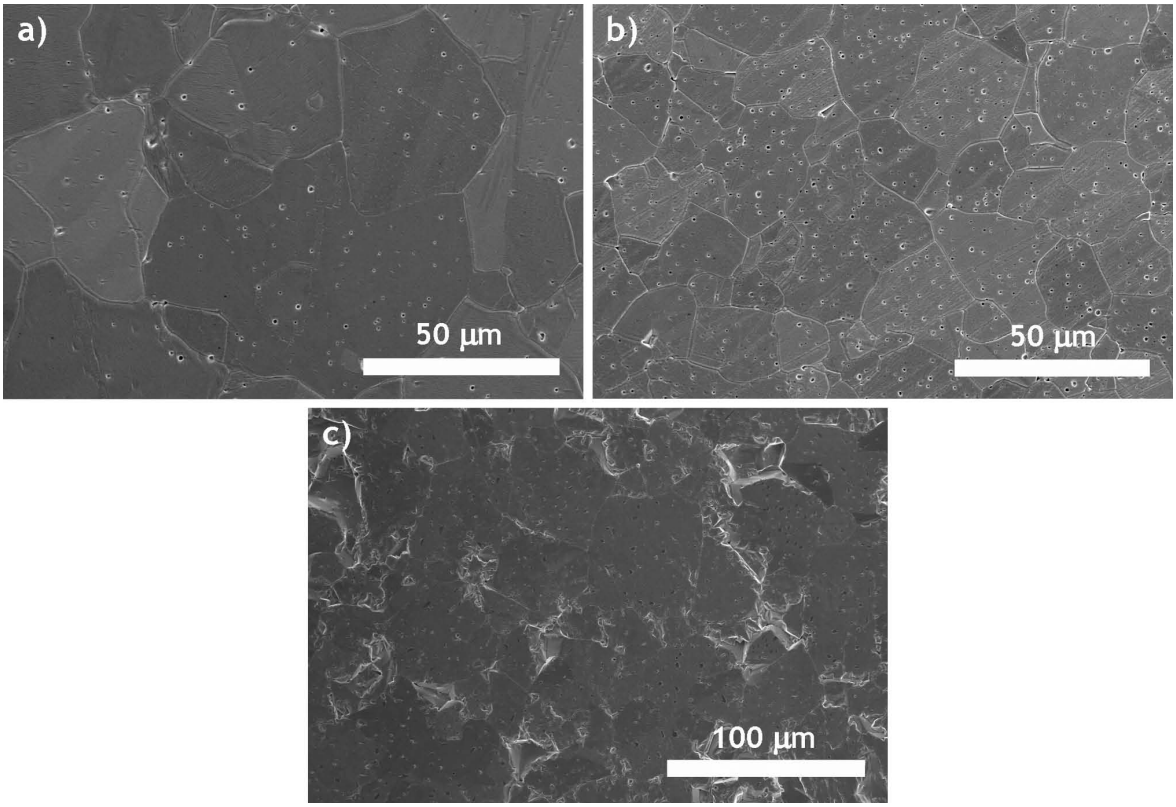

Fig. 10: SEM microphotographs of microstructure of samples prepared from I200 powder sintered at 1300 °C: a) PF, water; b) PF, propanol; c) ISO.

Possible ways of inhibiting the grain growth in BTO include the addition of small amounts of inhibitors e.g. Y_2O_3 [30, 31], Al_2O_3 [32], TiO_2 [33], or application of a different sintering technique such as SPS [8]. Some preliminary tests on either grain growth inhibitors and SPS sintering have been performed, and the latter solution has proven more effective. For the test, the sample filter-pressed from the water suspension of I100 powder was chosen because it showed the most favourable pore size distribution (Fig. 4b). The SPS-sintered sample showed some level of translucency related to its high density. The microstructure of the fracture surface of the sample filter-

pressed from the water suspension of I100 powder and sintered at 1100 °C for 5 min using the SPS method mostly consisted of sub-micrometric grains (Fig. 11). The relative density of the sample was 99.18 ± 0.20 %, which was the highest result achieved during the studies. However, the amount of remaining pores was still too high for transparent material. The conclusions presented above were confirmed by transmittance measurements (Fig. 12).

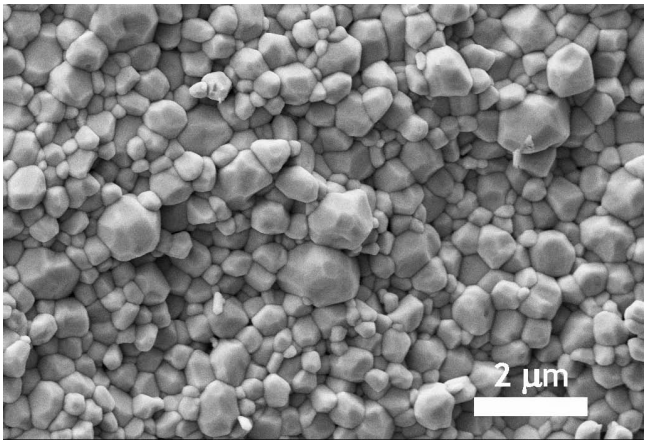

Fig. 11: Microstructure of sample filter pressed from water suspension of I100 powder sintered using SPS method.

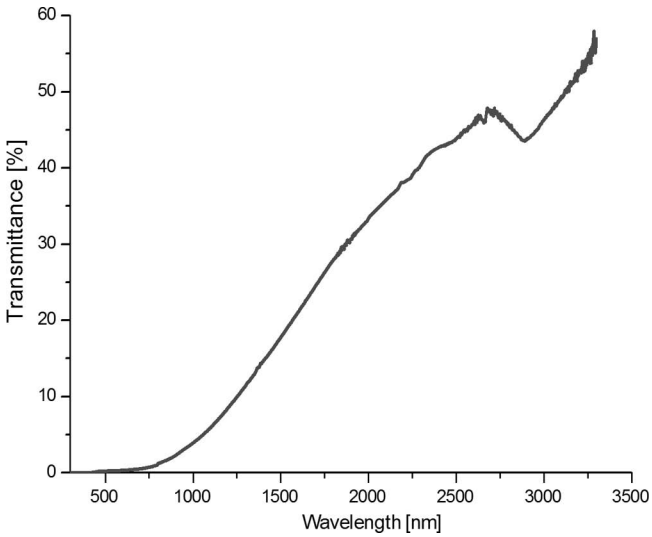

Fig. 12: Transmittance of sample sintered using SPS (I100, PF, water).

XRD analysis of selected, densified samples made of all powders revealed that no phase transformation took place and they consisted of tetragonal barium titanate phase. Maximum transmittance of the SPS sample was approx. 55 % at a wavelength of 3300 nm, and the transmittance in a visual region i.e. 380 – 780 nm was below 1 %. The apparent density and transmittance of the BTO sample were comparable to those obtained by Liu *et al.* with the high-pressure SPS method [8]. The main difference between those two studies was grain size, which was about 100 – 200 nm in the case of high-pressure SPS and 300 nm – 1 µm in the present study. Probably for that reason and because of birefringence shown the sample, the tetragonal BTO sample prepared by means of filter pressing was practically opaque in vis region, while the one prepared by Liu *et al.* exhibited transmittance of approx. 30 %.

The filter-pressed sample also exhibited an absorption peak at 2900 nm but it was much lower than that of the BTO prepared in the other work. The peak was attributed by Liu to stretching vibration of OH- groups [8], and since filter-pressed BTO consisted of larger grains and thus had a smaller surface area of grain boundaries, the number of such groups should be lower than in the case of polycrystal consisting of nanometric grains. To conclude, this preliminary test showed that it was possible to both reduce grain size and increase density of BTO prepared by means of filter pressing followed by sintering with the SPS method. Possible enhancement of these parameters requires further studies on SPS sintering.

IV. Conclusions

Dispersion of the fine barium titanate powders in water using combination of ammonium polymethacrylate and TMAH (pH 12) was effective, which was evidenced by the high absolute zeta potential values obtained. Aqueous suspensions of the fine barium titanate powders were generally composed of smaller particles than the propanol suspensions, which in turn led to significant differences in the pore size distribution of materials formed by means of pressure filtration. The pressure filtration method applied to aqueous suspensions of fine barium titanate powders led to the production of materials with narrow pore size distributions.

In most cases, modal pore diameters and total pore volume were smaller than those observed in materials prepared by means of cold isostatic pressing at 120 MPa. Sintering of the filter-pressed samples started at 900 – 950 °C, and they reached their highest densities at 1300 °C or 1350 °C. Abnormal grain growth and related to it pore entrapment limited final density of the samples to approx. 98 %. It was shown that further densification and restriction of the grain size was possible by sintering of the filter-pressed sample with the SPS method. Transmittance of samples prepared in this way reached 55 % in NIR region.

Acknowledgements

The work was financially supported by the Foundation for Polish Science co-financed by the Regional Development Fund of the European Union under the project POMOST/2013 – 7/14.

The authors would like to thank Dr Jarosław Woźniak for the SPS sintering.

References

1 Haertling, G.H.: Ferroelectric ceramics: History and technology. *J. Am. Ceram. Soc.*, **82**, 797 – 818, (1999).

2 Levinson, L.M.: Electronic Ceramics, Properties, Devices, and Applications, Marcel Dekker, New York, 1988.

3 Haertling, G.H., Land, C.E.: Hot-pressed (Pb,La)(Zr,Ti)O_3 ferroelectric ceramics for electrooptic applications, *J. Am. Ceram. Soc.*, **54**, 1 – 11, (1971).

4 Wu, Y.J., Wang, N., Wu, S.Y, Chen, X.M.: Transparent barium strontium titanate ceramics prepared by spark plasma sintering, *J. Am. Ceram. Soc.*, **94**, 1343 – 1345, (2011).

5 Li, F., Kwok, K-W.: $K_{0.5}Na_{0.5}NbO_3$-based lead-free transparent electro-optic ceramics prepared by pressureless sintering, *J. Am. Ceram. Soc.*, **96**, 3557 – 3562, (2013).

6 Li, F., Kwok, K-W.: Fabrication of transparent electro-optic $(K_{0.5}Na_{0.5})_{1-x}Li_xNb_{1-x}Bi_xO_3$ lead free ceramics, *J. Eur. Ceram. Soc.*, **33**, 123 – 130, (2013).

7 Shimooka, H., Kohiki, S., Kobayashi, T., Kuwabara, M.: Preparation of translucent barium titanate ceramics from sol-gel-derived transparent monolithic gels. *J. Mater. Chem.*, **10**, 1511 – 1512, (2000).

8 Liu, J., Shen, Z., Yao, W., Zhao, Y., Mukherjee, A.A.: Visible and infrared transparency in lead-free bulk $BaTiO_3$ and $SrTiO_3$ nanoceramics, *Nanotechnology*, **21**, 075706, (2010).

9 Groza, J.R.: Nanocrystalline powder consolidation methods, in: Nanostructured materials. Processing, properties, and potential applications. William Andrew Publishing/Noyes New York, 2002.

10 Hirata, Y., Nakamura, M., Miyamoto, M., Tanaka, Y., Wang, X.H.: Colloidal condensation of ceramic nanoparticles by pressure filtration, *J. Am. Ceram. Soc.*, **89**, 1883 – 1889, (2006).

11 Zych, Ł., Haberko, K.: Filter pressing and sintering of a zirconia nanopowder. *J. Eur. Ceram. Soc.*, **26**, 373 – 378, (2006).

12 Bergstrom, L., Shinozaki, K., Tomiyama, H., Mizutani, N.: Colloidal processing of a very fine $BaTiO_3$ powder – effect of particle interactions on the suspension properties, consolidation, and sintering behavior, *J. Am. Ceram. Soc.*, **80**, 291 – 300, (1997).

13 Gomez-Yanez, C., Balmori-Ramirez, H., Martinez, F.: Colloidal processing of $BaTiO_3$ using ammonium polyacrylate as dispersant, *Ceram. Int.*, **26**, 609 – 616, (2000).

14 Shen, Z-G., Chen, J-F., Zou, H-K., Yun, J.: Dispersion of nanosized aqueous suspensions of barium titanate with ammonium polyacrylate, *J. Colloid. Interf. Sci.*, **275**, 158 – 164, (2004).

15 Song, Y-L., Liu, X-L., Zhang, J-Q., Zou, X-Y., Chen, J-F.: Rheological properties of nanosized barium titanate prepared by HGRP for aqueous tape casting, *Powder Technol.*, **155**, 26 – 32, (2005).

16 Polotai, A., Breece, K., Dickey, E., Randall, C., Ragulya, A.: A novel approach to sintering nanocrystalline barium titanate ceramics, *J. Am. Ceram. Soc.*, **88**, 3008 – 3012, (2005).

17 Vinothini, V., Singh, P., Balasubramanian, M.: Optimization of barium titanate nanopowder slip for tape casting, *J. Mater. Sci.*, **41**, 7082 – 7087, (2006).

18 Santacruz, I., Nieto, M.I., Binner, J., Moreno, R.: Wet forming of concentrated nano-$BaTiO_3$ suspensions, *J. Eur. Ceram. Soc.*, **29**, 881 – 886, (2009).

19 Santacruz, I., Binner, J., Nieto, M.I., Moreno, R.: Dispersion and rheology of aqueous suspensions of nanosized $BaTiO_3$, *Int. J. Appl. Ceram. Technol.*, **7**, E135 – 143, (2010).

20 Ciofani, G., Danti, S., Moscato, S., Albertazzi, L., D'Alessandro, D., Dinucci, D., *et al.*: Preparation of stable dispersion of barium titanate nanoparticles: potential applications in biomedicine, *Colloid. Surface-B*, **76**, 535 – 543, (2010).

21 Nikumbh, A.K., Adhyapak, P.V.: Influence of preparation route and slip casting conditions on titania and barium titanate ceramics, *Particuology*, **10**, 371 – 383, (2012).

22 Ferreira, J.M.F., Olhero, S.M., Kaushal, A.: Is the ubiquitous presence of barium carbonate responsible for the poor aqueous processing ability of barium titanate? *J. Eur. Ceram. Soc.*, **22**, 2509 – 2517, (2013).

23 Jean, J-H., Wang, H-R.: Dispersion of aqueous barium titanate suspensions with ammonium salt of poly(methacrylic acid), *J. Am. Ceram. Soc.*, **81**, 1589 – 1599, (1998).

24 Blanco-Lopez, M.C., Rand, B., Riley, F.L.: The properties of aqueous phase suspensions of barium titanate, *J. Eur. Ceram. Soc.*, **17**, 281 – 287, (1997).

25 Blanco-Lopez, M.C., Fourlaris, G., Riley, F.L.: Interaction of barium titanate powders with an aqueous suspending medium, *J. Eur. Ceram. Soc.*, **18**, 2183 – 2192, (1998).

26 Boschini, F., Rulmont, A., Cloots, R., Moreno, R.: Colloidal stability of aqueous suspensions of barium zirconate, *J. Eur. Ceram. Soc.,* **25**, 3195 – 3201, (2005).

27 Krell, A., Blank, P., Ma, H., Hutzler, T., Nebelung, M.: Processing of high-density submicrometer Al_2O_3 for new applications, *J. Am. Ceram. Soc.*, **86**, 546 – 553, (2003).

28 O, Y.T., Koo, J.B., Hong, K.J., Park, J.S., Shin, D.C.: Effect of grain size on transmittance and mechanical strength of sintered alumina, *Mat. Sci. Eng. A-Struct.*, **374**, 191 – 195, (2004).

29 Vallar, S., Houivet, D., El Fallah, J., Kervadec, D., Haussonne, J-M.: Oxide slurries stability and powder dispersion: Optimization with zeta potential and rheological measurements. *J. Eur. Ceram. Soc.*, **19**, 1017 – 1021, (1999).

30 Matsuo, Y., Sasaki, H., Exaggerated grain growth in liquid-phase sintering of $BaTiO_3$, *J. Am. Ceram. Soc.*, **54**, 471, (1971).

31 Hennings, D.F.K., Janssen, R., Reynen, P.J.L.: Control of liquid-phase-enhanced discontinuous grain growth in barium titanate, *J. Am. Ceram. Soc.*, **70**, 23 – 27, (1987).

32 Pu, Y., Yang, W., Chen, S.: Influence of rare earths on electric properties and microstructure of barium titanate ceramics, *J. Rare. Earth*, **25**, 154 – 157, (2007).

33 Lee, J.K., Hong, K.S.: Revisit to the origin of grain growth anomaly in yttria-doped barium titanate, *J. Am. Ceram. Soc.*, **84**, 1745 – 1749, (2001).

34 Fisher, J.G., Lee, B.K., Brancquart, A., Choi, S.Y., *et al.*: Effect of Al_2O_3 dopant on abnormal grain growth in $BaTiO_3$, *J. Eur. Ceram. Soc.*, **25**, 2033 – 2036, (2005).

35 Yoo, Y.S., Kim, H., Kim, D.Y.: Effect of SiO_2 and TiO_2 addition on the exaggerated grain growth of $BaTiO_3$, *J. Eur. Ceram. Soc.*, **17**, 805 – 811, (1997).